



ELSEVIER

Superlattices and Microstructures 33 (2003) 347–356

Superlattices
and Microstructures

www.elsevier.com/locate/jnlabr/yspmi

Curved two-dimensional electron gases

Axel Lorke^{a,*}, Stefan Böhm^b, Werner Wegscheider^c

^a*Institut für Physik, Universität Duisburg-Essen, Lotharstr. 1, 47048 Duisburg, Germany*

^b*Center for NanoScience and Sektion Physik, Ludwig-Maximilians-Universität-München, Geschwister-Scholl-Platz 1, 80539 Munich, Germany*

^c*Walter-Schottky-Institut der TU München, Am Coulombwall, 85747 Garching, Germany*

Accepted 5 February 2004

Abstract

A method is introduced which makes it possible to fabricate non-planar two-dimensional electron gases. Making use of the “epitaxial lift-off” process, patterned, gated and contacted heterostructures are transferred from their crystalline substrate onto small glass tubes with diameters of a few millimeters. The transport properties of two-dimensional electron gases inside these curved semiconductor films are characterized by low-temperature magnetoresistance measurements. In the longitudinal resistance we find weak Shubnikov–de Haas oscillations, which are periodic in B^{-1} . The transverse resistance exhibits well-developed quantum Hall plateaus at low magnetic fields. At high fields, we observe a pronounced breakdown of the Hall effect. The experimental results are compared with simple theoretical models.

© 2004 Elsevier Ltd. All rights reserved.

Keywords: Epitaxial lift-off; Quantum Hall effect; Curved electron gases

1. Introduction

In the late 1960s to the early 1970s it was discovered that electron systems at semiconductor interfaces have unique optical and transport properties because of their *two-dimensional* nature [1–3]. Ever since (with only few exceptions) the label “two-dimensional” implied that these electron systems were planar or flat. Experimentally, this appears to be natural, considering that two-dimensional electron gases (2DEGs) are usually realized at nearly atomically smooth interfaces of single-crystalline semiconductors.

* Corresponding author.

E-mail address: axel.lorke@uni-duisburg.de (A. Lorke).

Mathematically, however, two-dimensional manifolds can very well be curved in three-dimensional space. Indeed, one of the first theoretical treatments of the quantum Hall effect in 2DEGs used a cylindrical geometry as a starting point [4].

Experimentally, a non-planar geometry is difficult to achieve, and only recently first reports on the realization of 2DEGs with complex topologies have been published. One approach is the overgrowth of crystalline facets, realized either by etching [5] or by in situ cleaving [6]. Another method makes use of built-in strain in lattice-mismatched heterostructures, which leads to a curling up of under-etched films [7].

Here, we introduce a method, which allows one to lift-off thin films of patterned, gated and contacted heterostructures, containing a high-mobility 2DEG. Because of the flexibility of the thin film it is then possible to transfer the heterostructure onto a cylindrical substrate and thus realize a curved two-dimensional electron gas.

2. Sample preparation

The heterostructures were grown by molecular beam epitaxy. Starting from a semi-insulating GaAs(100) substrate, a 500 nm thick GaAs smoothing layer was deposited, followed by 100 nm AlAs, which serves as a sacrificial layer for the “epitaxial lift-off” process (see below). A 10 nm thick GaAs layer serves to protect the following quantum well structure after the lift-off. The quantum well structure consists of 15 nm GaAs, embedded in $\text{Al}_{0.33}\text{Ga}_{0.67}\text{As}$ barrier layers. The top barrier is 130 nm thick and contains a Si δ -dopig layer, 30 nm away from the quantum well. The bottom barrier layer has a thickness of 150 nm. Finally, the heterostructure is capped by another 10 nm GaAs protective layer.

The transfer of the heterostructure onto a non-planar surface is based on the so-called “epitaxial lift-off” method [8–10], which relies on the extremely selective etching of AlAs by hydrofluoric acid. Beyond the actual lift-off process, we had to face two additional challenges, which are associated with the transfer onto a cylindrical substrate. First, since lithography on curved substrates is not possible using standard methods, the measuring geometry (a Hall bar), the gate and the ohmic contacts had to be defined before the lift-off (“preprocessing”). Secondly, the stiff protective wax layer [8, 10], which usually supports the semiconductor film during transfer onto a new substrate, had to be removed so that the film could adjust itself to the cylindrical surface. This, together with the metallic patterns from the preprocessing, made the transfer extremely difficult.

The processing steps are schematically shown in Fig. 1. Using standard optical lithography, first the source, the drain and the voltage probe contacts are defined (Fig. 1(a)). These consist of a AuGe/Ni layer and are annealed at 400 °C under an Ar:H atmosphere. Next, a 20 nm thick NiCr gate electrode is evaporated (Fig. 1(b)). The resist structure that will define the actual Hall geometry is patterned in the following step (Fig. 1(c)). It is not possible, however, to etch the Hall bar in the preprocessing steps, since the fine structures would make the following lift-off and transfer process impossible. A protective wax layer of a few hundred microns thickness is deposited (Fig. 1(d)) to protect the structure during the following HF etching step. When the AlAs sacrificial layer is etched away, the complete heterostructure containing the 2DEG can be lifted off. The next processing step, during which the supporting wax is removed and the extremely fragile semiconductor film is transferred onto a small glass tube, is the most challenging. The lift-off structure is placed onto a water

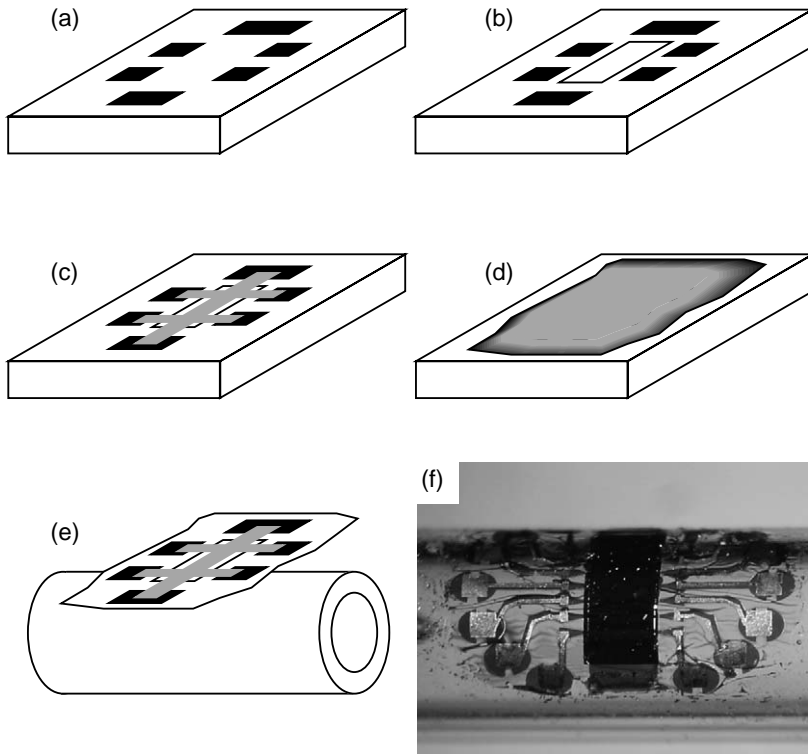


Fig. 1. Processing steps for transferring a patterned and gated heterostructure onto a curved substrate. For details, see text. (f) shows a photograph of a completely processed sample on a glass tube of 1.1 mm radius.

surface where it stays afloat because of surface tension. Then, trichloroethylene is carefully pumped (through four pipettes) across the floating structure to remove the wax. Photoresist is almost insoluble in trichloroethylene, so that the predefined Hall bar pattern is not affected. Now, from below the water surface, a glass tube is slowly raised (Fig. 1(e)). As the preprocessed semiconductor film is lifted above the surface by the glass tube, it takes on the cylindrical shape of the tube and adheres to the glass surface by van der Waals forces [8–10]. After a drying step to improve adhesion, the Hall bar structure can be etched, using the predefined photoresist pattern. A photograph of the fully processed sample is shown in Fig. 1(f). Details of the procedure summarized here can be found in [11].

Using this method, curved 2DEGs with radii down to 1 mm can be realized and characterized at low temperatures and high magnetic fields.

3. Curved 2DEGs in high magnetic fields

3.1. The bulk picture

Even though there is only little experimental work on non-planar electron gases in high magnetic fields, there are a number of theoretical papers dealing with this topic [12–16].

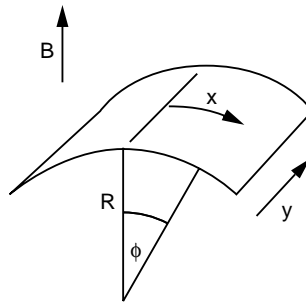


Fig. 2. Geometry of a curved sample in a homogeneous magnetic field B .

For strictly two-dimensional electron systems (more precisely: when the spatial quantization in the third dimension, ΔE_z , is much larger than the magnetic confinement $\hbar\omega_c$) the problem is equivalent to that of a planar geometry with a strongly varying magnetic field, which has been considered in [17, 18]. Here, we will only give a short introduction into the topic and refer to the above references for a more detailed discussion.

The geometry of a curved 2DEG in a homogeneous magnetic field is shown in Fig. 2. We assume a strictly two-dimensional electron gas and neglect spin splitting, so that the in-plane component of the magnetic field does not influence the energetic structure of the system. The problem then reduces to solving the Schrödinger equation

$$\frac{1}{2m}(-i\hbar\nabla + e\mathbf{A})^2\psi = E\psi$$

in two dimensions. Taking the magnetic field $\mathbf{B} = (0, 0, B \cos(\phi))$ and the vector potential in asymmetric gauge $\mathbf{A} = (0, BR \sin(\phi), 0)$ we find

$$-\frac{\hbar^2}{2m} \frac{\partial^2 \psi}{\partial x^2} + \frac{1}{2} m \omega_c^2 \left(R \sin \frac{x}{R} - \frac{\hbar k_y}{eB} \right)^2 \psi = E \psi. \tag{1}$$

Here, $\omega_c = eB/m$ is the cyclotron frequency and k_y is the wave vector of motion in y -direction, which can be separated within the asymmetric gauge. The quantities x , R and ϕ are given in Fig. 2. Note that for $R \rightarrow \infty$ Eq. (1) reduces to the common expression (in Landau gauge) for a flat 2DEG in a perpendicular magnetic field [19]

$$-\frac{\hbar^2}{2m} \frac{\partial^2 \psi}{\partial x^2} + \frac{1}{2} m \omega_c^2 (x - x_o)^2 \psi = E \psi, \tag{2}$$

with $x_o = \hbar k_y / eB$ being the apex of the (magnetic) confinement parabola. Eq. (1) can be simplified by introducing local coordinates around the minimum $x_m = R \arcsin(x_o/R)$ of the term in parenthesis

$$\sin \frac{x_m + x'}{R} - \frac{x_o}{R} = \sin \frac{x_m}{R} \underbrace{\cos \frac{x'}{R}}_{\approx 1} + \cos \frac{x_m}{R} \underbrace{\sin \frac{x'}{R}}_{\approx x'/R} - \frac{x_o}{R} \approx \frac{x'}{R} \cos \frac{x_m}{R}. \tag{3}$$

Here we have made the assumption that the local coordinate $x' \ll R$. Since the radius of curvature R is of the order of 1 mm whereas the local coordinate is relevant on the scale of

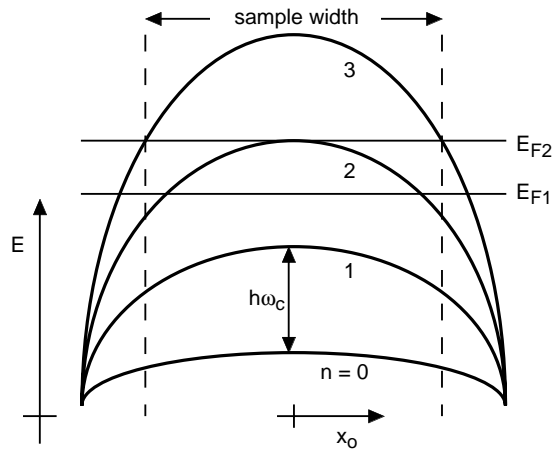


Fig. 3. Dispersion of Landau bands with different Landau indices n in a curved sample.

the magnetic length (≈ 25 nm at 1 T), this assumption is well justified. For a discussion of $x' \approx R$, see e.g., [13, 15, 17, 18].

From (1) and (3) follows

$$-\frac{\hbar^2}{2m} \frac{\partial^2 \psi}{\partial x'^2} + \frac{1}{2} m \left(\omega_c \cos \frac{x_m}{R} \right) (x' - x_m)^2 \psi = E \psi,$$

which is equivalent to Eq. (2), only with a rescaled effective magnetic field $B_{\text{eff}} = B \cos(x_m/R)$. In analogy to the solution of Eq. (2) [19] we find the energy dispersion of a curved 2DEG in cylindrical geometry [14]

$$\begin{aligned} E_n &= \left(n + \frac{1}{2} \right) \hbar \omega_c \cos \frac{x_m}{R} = \left(n + \frac{1}{2} \right) \hbar \omega_c \cos \left(\arcsin \frac{x_0}{R} \right) \\ &= \left(n + \frac{1}{2} \right) \hbar \omega_c \sqrt{1 - \frac{x_0^2}{R^2}}. \end{aligned}$$

The Landau levels, which are dispersionless in the planar case, now have a semielliptical dispersion as a function of $x_0 = \hbar k_y / eB$. This situation is sketched in Fig. 3.

The density of states will still oscillate as a function of the Fermi energy (cf. the two examples E_{F1} and E_{F2} in Fig. 3). Shubnikov–de Haas oscillations are therefore still expected in magnetotransport experiments. The non-vanishing density of states between the maximum energies $E_{n,\text{max}} = (n + 1/2)\hbar\omega_c$, however, leads to profound changes in the quantum Hall effect. For example, for a curved 2DEG, no localized states have to be assumed to explain the occurrence of Hall plateaus,—the density of states between the $E_{n,\text{max}}$ will fulfill a similar role [15].

3.2. The edge state picture

So far, we have discussed the energetic structure of a curved 2DEG in the bulk picture and neglected the edges of the sample. As in the planar case, the Landau bands will

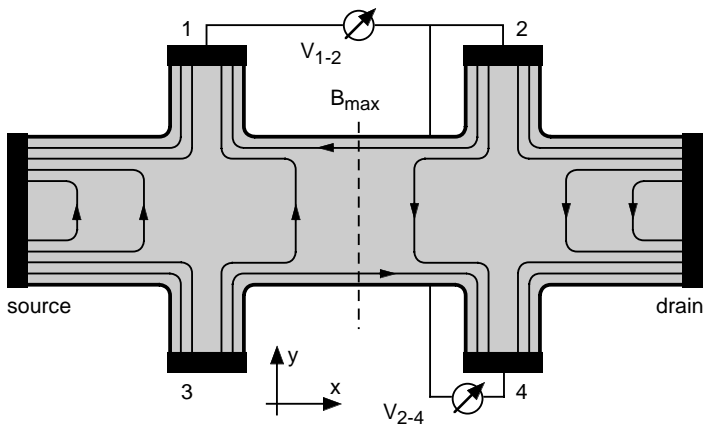


Fig. 4. Geometry of the current-carrying states in a sample with laterally varying magnetic field B_{eff} .

be bent upwards at the edges and intersect with the Fermi energy, forming so-called edge channels. In the simplest Landauer–Büttiker picture, the number of these edge channels will determine the longitudinal and transverse resistance under quantum Hall conditions [19]. In curved 2DEGs, however, the Landau bands will also intersect with the Fermi energy *in the interior* of the sample (see Fig. 3, E_{F1}).

A structure with interior, current-carrying states is sketched in Fig. 4. For simplicity, we have replaced the curved structure in a homogeneous field by a planar sample in a varying field $B_{\text{eff}}(x) = B_{\text{max}} \cos(x/R)$. The variation of B_{eff} is chosen such that the local filling factor is $\nu = 4$ at the source and drain contacts and $\nu = 2$ in the center region. The figure shows that the two additional edge states that leave the source and drain regions are reflected back (through the bulk current-carrying states) to their origin. In the Landauer–Büttiker formalism this means that they do not contribute to any of the voltages measured outside the source and drain. The longitudinal voltage V_{1-2} will therefore only be determined by the field in the region between the voltage probes 1 and 2. More detailed calculations suggest further that the longitudinal resistance $R_{xx} = V_{1-2}/I_{s-d}$ is given by the *maximum* field between the voltage probes.

The Hall resistance $R_{xy} = V_{2-4}/I_{s-d}$ is simply given by the number N of channels coming out of and going into the voltage probes ($N = 2$ for the situation in Fig. 4)

$$R_{xy} = \frac{h}{Ne^2}.$$

4. Experimental results

The samples are mounted in a liquid-He cryostat in the center of a superconducting solenoid, and the magnetotransport characteristics are investigated by standard 4-probe magnetoresistance measurements. The sample stage can be rotated in situ around the axis of the glass tube, making it possible to probe R_{xx} and R_{xy} at different positions with respect to the magnetic field orientation.

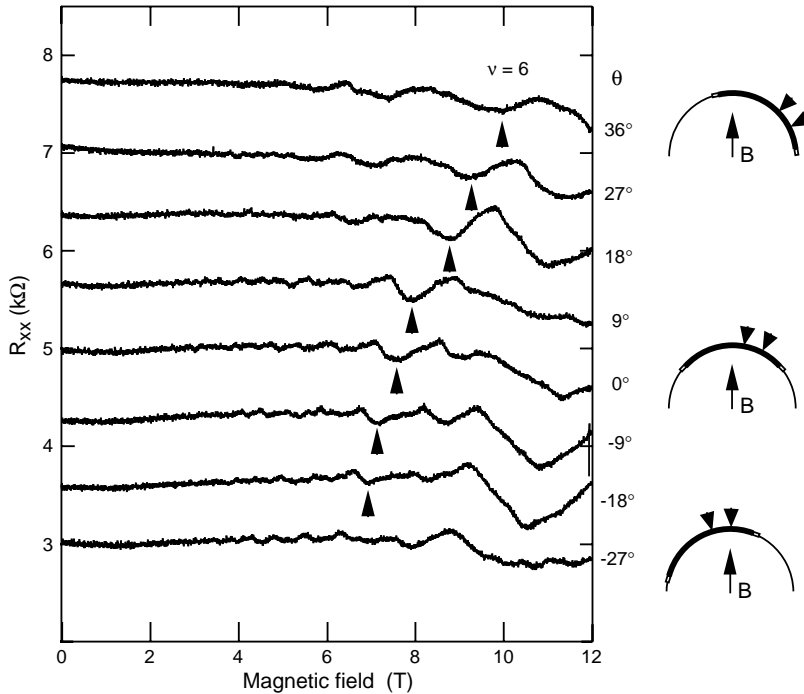


Fig. 5. Longitudinal resistance of sample A in a homogeneous magnetic field. Weak Shubnikov–de Haas oscillations are observed. Arrows mark the position of the filling factor $\nu = 6$. The position of the sample and the voltage probes (downward arrows) with respect to the magnetic field B are indicated on the right. Between consecutive measurements, the sample is rotated by approximately 9° . The radius of curvature is 1.1 mm, the length of the 2DEG (distance between source and drain) is 1.8 mm, the voltage probes are spaced by $370 \mu\text{m}$. Traces are offset for clarity.

Fig. 5 shows the longitudinal resistance of sample A as a function of the magnetic field for different sample orientations. The measurements exhibit a high zero-field resistance and a high noise level, which may be caused by microscopic ruptures in the lift-off film, a possible result of an imperfect transfer process. Still a number of conclusions can be drawn from Fig. 5.

As expected from the bulk picture of a curved 2DEG, weak Shubnikov–de Haas oscillations are observed. Within the experimental resolution of these and other (R_{xx} and R_{xy}) data [5], the oscillations are periodic in B^{-1} , just as in flat samples. This is somewhat surprising. When the Fermi energy is an integer multiple of $\hbar\omega_c$ in a flat 2DEG, the number of filled Landau levels will be integer, too. This may not be the case in a curved sample, as shown in Fig. 3, where for $E_F = E_{F1}$ the Landau bands $n = 0, 1$ are fully occupied, whereas the $n = 2$ band is partially filled at the sample edges. Indeed, calculations by Chaplik et al. [15, 16] show a deviation from the B^{-1} -periodicity in the Hall conductance. These calculations, however, were performed for a much smaller radius of curvature than the one used here. This may be the reason why we cannot resolve a deviation from the B^{-1} -periodicity in the present data.

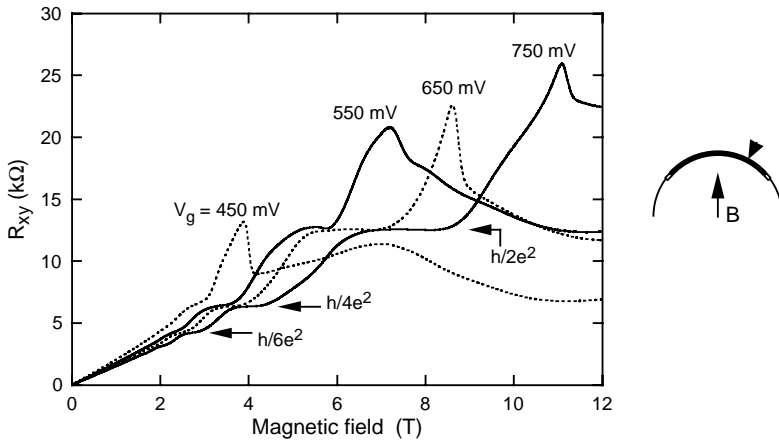


Fig. 6. Hall resistance of sample *B* for different gate voltages. The measurement geometry is indicated on the right. The radius of curvature is 1.1 mm, the distance between the source and drain is 1.8 mm.

The arrows in Fig. 5 indicate the minima corresponding to filling factor $\nu = 6$ for different tilt angles θ . The positions of these minima roughly shift with $\cos(\theta)$, as expected from the edge state picture, which suggests that the field $B_{\text{eff}} = B_{\text{max}} \cos(\theta)$ between the voltage probes determines the resistance. Measurements of R_{xx} with voltage probes that are further apart [11] show that it is indeed the maximum field (and not, e.g., the average field) which determines the minima of the oscillations: as long as B_{max} lies between the voltage probes, R_{xx} is not affected by θ . Only when the tilt angle is further increased, the minima start to shift.

Fig. 6 shows the Hall resistance of sample *B* for different gate voltages V_g . For $V_g = 750$ mV and $B < 10$ T, well-developed, quantized Hall plateaus are observed, which are again periodic in B^{-1} . For higher fields or lower gate voltages, however, strong deviations from the common quantum Hall characteristics develop. Instead of plateaus, pronounced maxima appear and the Hall voltage starts to decrease with increasing field. So far, we have no explanation for this unusual behavior. Detailed calculations within the Landauer–Büttiker formalism, e.g., could not reproduce the breakdown of the Hall voltage. Furthermore, because of the well-developed Hall plateaus at low fields, it is unlikely that the breakdown is the result of an ill-defined sample geometry, caused e.g., by inhomogeneities or cracks in the lift-off film.

A possible explanation may be the redistribution of carriers when a curved 2DEG is subjected to a high magnetic field. In a flat sample, the Fermi energy oscillates as a function of the magnetic field in a saw-tooth pattern [19]. For a curved sample with a locally varying B_{eff} , this would lead to a non-equilibrium situation, i.e. a locally varying E_F . A constant Fermi energy across the sample can only be maintained by a redistribution of carriers. This is similar to the reconstruction of the Landau level structure at the edge of a flat sample [20]. The extent of the carrier redistribution is given by the interplay between magnetic quantization and electron–electron interaction. The trend observed in Fig. 6 supports this picture: for lower carrier densities and thus lower electron–electron

interaction, the breakdown of the Hall effect takes place at lower magnetic fields. A more complete, self-consistent treatment of the problem is necessary, however, to assess how much the redistribution of carriers really affects the transport properties and whether it can indeed explain the observed breakdown of the Hall effect.

5. Summary

In conclusion, we have developed a method to lift off patterned and preprocessed heterostructures from their crystalline substrates and transfer them onto almost arbitrary substrates. Using this technique and employing a small glass tube as a support, we have fabricated curved two-dimensional electron gases, patterned into a Hall bar geometry. At low temperatures and high magnetic fields the longitudinal resistance R_{xx} exhibits Shubnikov–de Haas oscillations, which are determined by the maximum effective field between the voltage probes. Pronounced maxima and a breakdown of the Hall voltage are observed in the transverse magnetoresistance R_{xy} . Whereas the general behavior of R_{xx} can be understood using simple edge or bulk pictures of magnetotransport in a curved 2DEG, the observed features in the Hall resistance remain unexplained.

Acknowledgements

Our knowledge of two-dimensional systems, which is the basis of the present work, has to a large extent been developed in a long, fruitful, stimulating and pleasant collaboration with Jörg Kotthaus, one of the pioneers in this field. We would like to thank him for his continuous support.

We would also like to thank Alik Chaplik, Achim Wixforth, Martin Rotter and Thomas Klühspies for valuable discussions and technical assistance.

Financial support by the Deutsche Forschungsgemeinschaft through grant LO 705/1 is gratefully acknowledged.

References

- [1] A.B. Fowler, F.F. Fang, W.E. Howard, P.J. Stiles, Phys. Rev. Lett. 16 (1966) 901.
- [2] F. Stern, Phys. Rev. Lett. 18 (1967) 546.
- [3] J.P. Kotthaus, G. Abstreiter, G.F. Koch, Phys. Rev. Lett. 34 (1975) 151.
- [4] R.B. Laughlin, Phys. Rev. B 23 (1981) 5632.
- [5] M.L. Leadbeater et al., Phys. Rev. B 52 (1995) R8629.
- [6] M. Grayson et al., Physica E (submitted for publication) [cond-mat/0308557](#).
- [7] A. Vorob'ev, V. Prinz, V. Preobrazhenskii, B. Semyagin, Jpn. J. Appl. Phys. 42 (2003) L7 and references therein.
- [8] E. Yablonovitch, D.M. Hwang, T.J. Gmitter, L.T. Florez, J.P. Harbison, Appl. Phys. Lett. 56 (1990) 2419.
- [9] P. Demeester, I. Pollentier, P. de Dobbelaere, C. Brys, P. Van Daele, Semicond. Sci. Technol. 8 (1993) 1124 and references therein.
- [10] M. Rotter, C. Rocke, S. Böhm, A. Lorke, A. Wixforth, W. Ruile, L. Korte, Appl. Phys. Lett. 70 (1997) 2097.
- [11] S. Böhm, Dissertation, LMU München, 2002.
- [12] C.L. Foden, M.L. Leadbeater, J.H. Burroughes, M. Pepper, J. Phys. Condens. Matter 6 (1994) L127.
- [13] C.L. Foden, M.L. Leadbeater, M. Pepper, Phys. Rev. B 52 (1995) R8646.
- [14] L.I. Magarill, D.A. Romanov, A.V. Chaplik, JETP Lett. 64 (1996) 460.

- [15] A.V. Chaplik, L.I. Magarill, D.A. Romanov, *Physica B* 249–251 (1998) 377.
- [16] A.V. Chaplik, L.I. Magarill, D.A. Romanov, *Phys. Low-Dim. Struct.* 1–2 (1998) 17.
- [17] J.E. Müller, *Phys. Rev. Lett.* 68 (1992) 385.
- [18] E. Hofstetter, J.M.C. Taylor, A. MacKinnon, *Phys. Rev. B* 53 (1996) 4676.
- [19] See, e.g. J.H. Davies, *The Physics of Low-Dimensional Semiconductors*, Cambridge University Press, 1998.
- [20] D.B. Chklovskii, B.I. Shklovskii, L.I. Glazman, *Phys. Rev. B* 46 (1992) 4026.